



OPEN ACCESS

EDITED BY

Chunxue Bai,
Fudan University, China

REVIEWED BY

Gianna Camiciottoli,
University of Florence– University Hospital
Careggi-Florence, Italy
Grace Hyun Kim,
UCLA Health System, United States

*CORRESPONDENCE

Philip Konietzke
✉ p.konietzke@gmx.de

RECEIVED 12 March 2023

ACCEPTED 22 June 2023

PUBLISHED 18 July 2023

CITATION

Konietzke P, Brunner C, Konietzke M,
Wagner WL, Weinheimer O, Heußel CP,
Herth FJF, Trudzinski F, Kauczor H-U and
Wielpütz MO (2023) GOLD stage-specific
phenotyping of emphysema and airway disease
using quantitative computed tomography.
Front. Med. 10:1184784.
doi: 10.3389/fmed.2023.1184784

COPYRIGHT

© 2023 Konietzke, Brunner, Konietzke, Wagner,
Weinheimer, Heußel, Herth, Trudzinski, Kauczor
and Wielpütz. This is an open-access article
distributed under the terms of the [Creative Commons Attribution License \(CC BY\)](https://creativecommons.org/licenses/by/4.0/). The
use, distribution or reproduction in other
forums is permitted, provided the original
author(s) and the copyright owner(s) are
credited and that the original publication in this
journal is cited, in accordance with accepted
academic practice. No use, distribution or
reproduction is permitted which does not
comply with these terms.

GOLD stage-specific phenotyping of emphysema and airway disease using quantitative computed tomography

Philip Konietzke^{1,2,3*}, Christian Brunner^{1,2,3}, Marilisa Konietzke^{1,2},
Willi Linus Wagner^{1,2,3}, Oliver Weinheimer^{1,2,3},
Claus Peter Heußel^{1,2,3}, Felix J. F. Herth^{2,4}, Franziska Trudzinski^{2,4},
Hans-Ulrich Kauczor^{1,2,3} and Mark Oliver Wielpütz^{1,2,3}

¹Department of Diagnostic and Interventional Radiology, University Hospital of Heidelberg, Heidelberg, Germany, ²Translational Lung Research Center Heidelberg (TLRC), German Center for Lung Research (DZL), University of Heidelberg, Heidelberg, Germany, ³Department of Diagnostic and Interventional Radiology with Nuclear Medicine, Thoraxklinik at University of Heidelberg, Heidelberg, Germany, ⁴Department of Pulmonology, Thoraxklinik at University of Heidelberg, Heidelberg, Germany

Background: In chronic obstructive pulmonary disease (COPD) abnormal lung function is related to emphysema and airway obstruction, but their relative contribution in each GOLD-stage is not fully understood. In this study, we used quantitative computed tomography (QCT) parameters for phenotyping of emphysema and airway abnormalities, and to investigate the relative contribution of QCT emphysema and airway parameters to airflow limitation specifically in each GOLD stage.

Methods: Non-contrast computed tomography (CT) of 492 patients with COPD former GOLD 0 COPD and COPD stages GOLD 1–4 were evaluated using fully automated software for quantitative CT. Total lung volume (TLV), emphysema index (EI), mean lung density (MLD), and airway wall thickness (WT), total diameter (TD), lumen area (LA), and wall percentage (WP) were calculated for the entire lung, as well as for all lung lobes separately. Results from the 3rd–8th airway generation were aggregated (WT_{3–8}, TD_{3–8}, LA_{3–8}, WP_{3–8}). All subjects underwent whole-body plethysmography (FEV1%pred, VC, RV, TLC).

Results: EI was higher with increasing GOLD stages with 1.0±1.8% in GOLD 0, 4.5±9.9% in GOLD 1, 19.4±15.8% in GOLD 2, 32.7±13.4% in GOLD 3 and 41.4±10.0% in GOLD 4 subjects ($p < 0.001$). WP_{3–8} showed no essential differences between GOLD 0 and GOLD 1, tended to be higher in GOLD 2 with 52.4±7.2%, and was lower in GOLD 4 with 50.6±5.9% ($p = 0.010 - p = 0.960$). In the upper lobes WP_{3–8} showed no significant differences between the GOLD stages ($p = 0.824$), while in the lower lobes the lowest WP_{3–8} was found in GOLD 0/1 with 49.9±6.5%, while higher values were detected in GOLD 2 with 51.9±6.4% and in GOLD 3/4 with 51.0±6.0% ($p < 0.05$). In a multilinear regression analysis, the dependent variable FEV1%pred can be predicted by a combination of both the independent variables EI ($p < 0.001$) and WP_{3–8} ($p < 0.001$).

Conclusion: QCT parameters showed a significant increase of emphysema from GOLD 0–4 COPD. Airway changes showed a different spatial pattern with higher values of relative wall thickness in the lower lobes until GOLD 2 and subsequent lower values in GOLD 3/4, whereas there were no significant differences in the upper lobes. Both, EI and WP_{5–8} are independently correlated with lung function decline.

KEYWORDS

chronic obstructive pulmonary disease (COPD), quantitative CT (QCT), GOLD stages, airway disease, lung emphysema

Highlights

1. QCT showed significant differences between GOLD 0–4.
2. Airway parameters indicate a transient inflammatory response in GOLD 2 leading to airway destruction in GOLD 4.
3. QCT could detect spatial differences between upper and lower lung lobes.
4. FEV1%pred appears to be predicted by a linear combination of the independent variables EI and WP₃₋₈.

Introduction

Chronic obstructive pulmonary disease (COPD) is the fourth leading cause of death worldwide and typically results from prolonged inhalation of noxious particles (1, 2). The diagnosis is made by symptoms and pulmonary function testing (PFT), and severity is commonly classified according to the GOLD criteria (3). Early detection of the disease is of great interest because airway disease is potentially reversible with smoking cessation or appropriate treatment, thereby delaying irreversible disease progression (4, 5). PFT play a central role in COPD diagnosis, yet its role in early diagnosis and reproducibility are limited. FEV1 is often normal until more than 30% of lung tissue are damaged or more than 75% small airways are obstructed (6, 7) due to compensation mechanisms of the lungs. Koo et al. showed that airway changes such as thickened bronchiolar walls, decreased number of bronchioles, and narrowed bronchiolar lumen occur earlier than the presence of emphysema in patients with mild GOLD COPD (8).

The use of computed tomography (CT) has led to better characterization of disease heterogeneity across patients at risk of COPD (former GOLD 0) to late stages with advanced emphysema. CT imaging allows deeper insights into different disease phenotypes and more accurate assessment of disease severity and distribution (9–11). Moreover, software-based post-processing (QCT) may detect and quantify the presence and type of emphysema by analysis of lung density (12–14). The assessment of airway disease is more challenging and less validated (12). QCT of small airways disease (SAD) is particularly challenging because CT measurements of airways are accurate and reproducible up to an diameter of approximately 2 mm, but those airways may serve as a surrogate for the smaller airways (15, 16). All these parameters are heavily influenced by technical factors such as scanner type, contrast material, slice thickness, kernel, and post-processing software. However, larger airways that can be visualized on CT allow conclusions about the status of smaller airways (16, 17). At present, larger studies on the quantitative contribution of emphysema and airways disease to airflow limitation are sparse.

Thus, we hypothesized that emphysema and airway abnormalities are independent factors determining airflow limitation in COPD, and that both have different systematic impact in different GOLD stages. In this work-up, we used QCT for GOLD-stage specific differential characterization of emphysema and airway abnormalities in a relatively large group of 522 patients with former GOLD 0 COPD and GOLD stages COPD 1–4 were examined with a comparable protocol on the same scanner.

Materials and methods

Patients

This retrospective study was approved by the institutional ethics committee (S-646/2016). The patient cohort was retrospectively recruited from the institutional imaging database. All adult patients who had an inspiratory CT scan between 08/2016 and 01/2020 at our chest-hospital were included if whole-body plethysmography was available within 45 days. The clinical exclusion criteria were pulmonary infections, lung tumors >1 cm, prior lung surgery, or volume-reducing procedures, and technical exclusion criteria were use of contrast media, image artifacts, missing or other reconstructions as I40f3 and I70f3, slice thickness of 1.25 mm, or errors in data export. All examinations were visually inspected for the absence of significant motion artifacts and inclusion of all parts of the chest by a senior chest radiologist.

All patients were diagnosed with COPD according to GOLD 2020 (18). In addition to subjects of the GOLD 1–4 categories, smokers and former smokers with no assignable GOLD category including the “former GOLD 0” were enrolled. The “former GOLD 0” group includes subjects with normal PFT in terms of FEV1/FVC (ratio between forced expiratory volume in 1 s and forced vital capacity) but with COPD-specific symptoms. Based on these criteria, 5 study groups (GOLD 0–4) were defined.

Whole-body plethysmography

All patients had whole-body plethysmography 0–45 days within the CT scan using reference values according to the Global Lung Initiative (19). In this study, vital capacity (VC), forced vital capacity (FVC), residual volume (RC), total lung capacity (TLC), forced expiratory volume in 1 s (FEV1), FEV1 predicted (FEV1%) and the ratio FEV1/FVC were used.

CT acquisition and reconstruction

Non-contrast CT (Somatom Definition AS64, Siemens Healthineers AG) was performed in supine position, as recommended for COPD (20). All patients were instructed and carefully monitored for a stable full automatically instructed inspiratory breath-hold before scanning. The CT scanner was routinely calibrated every 3 months for water and daily for air. Scans were performed in caudocranial direction with a dose-modulated protocol (Caredose4D, Siemens Healthineers AG) using a reference of 120 kV and 70 mA or 100 kV

and 117 mA (120/70//100/117 [kV/mA]; GOLD 0 = 28/95, GOLD 1 = 9/24, GOLD 2 = 44/71, GOLD 3 = 83/98, GOLD 4 = 16/24) at a collimation of 64×0.6 mm and a pitch of 1.45. The reconstructed slice thickness was 1.00 mm with 0.825 mm increment. For each patient, a set of two reconstructions was available, namely a medium soft reconstruction algorithm (I40f3) and the edge-enhancing reconstruction algorithm (I70f3).

Quantitative post-processing

The in-house software YACTA, a non-commercial scientific software, segmented the airway tree and lung lobes fully automated, using the I40f3 kernel for parenchymal analysis and the I70f3 kernel for airway analysis as previously published (21–26). The total lung volume (TLV), emphysema index (EI) and mean lung density (MLD) were calculated for the total lung and for all lung lobes separately (right upper (RUL), middle (RML), and lower (RLL) lobe, as well as left upper lobe (LUL), lingula (LLi) and left lower lobe (LLL)). The airway parameters wall thickness (WT), total diameter (TD), lumen area (LA), and wall percentage (WP) were analysed generation-based in the trachea (G_1), right and left main stem (G_2), lobar (G_3), segmental (G_4), and the subsegmental bronchi (G_{5-8}). Airway results were simplified by consolidating the generation-based results for the 3rd to 8th generation (G_{3-8}).

Statistical analysis

Statistical analyses were performed using R (R 3.3.2, Foundation for Statistical Computing) and SigmaPlot (Systat Software GmbH). Data are presented as mean \pm standard deviation. One-way analysis of variance (ANOVA), Tukey multiple pairwise-comparisons (Tukey Test), Spearman linear and multiple linear regression were used. Correlation coefficients were interpreted as follows: 0.00–0.10 (negligible), 0.10–0.39 (weak), 0.40–0.69 (moderate), 0.70–0.89 (strong), and 0.90–1.00 (very strong) (27). A value of $p < 0.05$ was considered statistically significant.

Results

Patient cohort and demographics

The final cohort included 522 patients out of 15,631. 10,358 patients were excluded because of contrast media application, 4,503 patients because of clinical exclusion criteria. 275 patients were excluded due to technical exclusion criteria significant motion artifacts (74), incomplete inclusion of all parts of the chest (28), invalid export from PACS system (12), slice thickness 1.25 mm (27), missing I70f3 reconstruction (77), other reconstructions as I40f3 (conventional filtered backprojection) (21), B40f (11) and B40s (18) kernel. The final cohort consisted of 492 patients, of whom 29 patients were diagnosed with GOLD 0, 34 with GOLD 1 COPD, 123 with GOLD 2 COPD, 196 with GOLD 3 COPD, and 40 with GOLD 4 COPD.

Patients with GOLD 0 COPD had the highest vital capacity (VC) with 3.6 ± 1.2 L and the lowest residual volume (RV) with 2.6 ± 0.8 L as

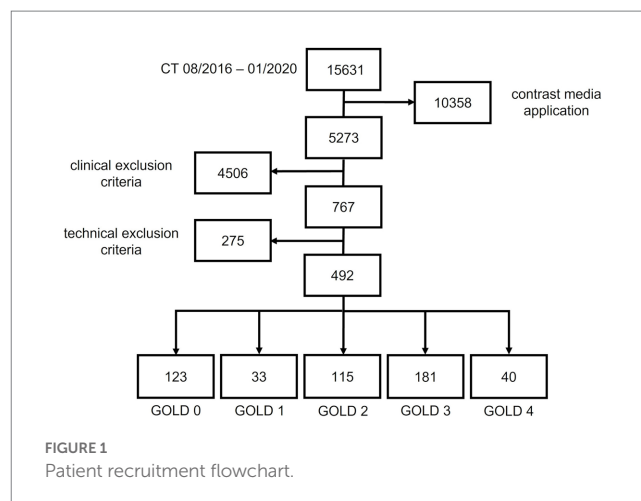


FIGURE 1
Patient recruitment flowchart.

well as the lowest total lung capacity (TLC) with 6.2 ± 1.4 L. RV and TLC were higher in each GOLD stage from GOLD 0 to 3, being slightly lower again at GOLD 4 (all $p < 0.001$). FEV1%pred was lower at each GOLD stage as per definition ($p < 0.001$) (Figure 1; Table 1).

GOLD stage-specific quantification of emphysema and airway disease

TLV was 5198 ± 1349 cm³ in GOLD 0, higher with 7405 ± 1366 cm³ in GOLD 3 ($p < 0.001$) and lower in GOLD 4 with 6892 ± 1292 cm³ ($p = 0.193$). Emphysema was measured with an EI of $1.17 \pm 1.8\%$ in GOLD 0 and of $4.5 \pm 9.9\%$ in GOLD 1 ($p = 0.564$). EI was higher with increasing GOLD stages with $19.4 \pm 15.8\%$ in GOLD 2 ($p < 0.05$), $32.7 \pm 13.4\%$ in GOLD 3 ($p < 0.05$), and $41.4 \pm 10.0\%$ in GOLD 4 ($p < 0.05$). Accordingly, MLD showed a comparable pattern, with -802 ± 38 HU in GOLD 0 and progressively lower values in GOLD 1 with -820 ± 32 HU ($p = 0.044$), in GOLD 2 with -850 ± 30 HU ($p < 0.05$), and in GOLD 3 with -872 ± 19 HU ($p < 0.05$), while the MLD was again slightly higher in GOLD 4 with -876 ± 14 HU ($p = 0.971$) (Figures 2, 3; Table 2).

WT₃₋₈ showed no essential differences between GOLD 0 and GOLD 1 with 1.17 ± 0.21 mm and 1.14 ± 0.16 mm ($p = 0.960$), respectively. In GOLD 2, it tended to be higher with 1.24 ± 0.24 mm ($p = 0.101$), while it was lower with 1.17 ± 0.19 mm in GOLD 3 ($p < 0.05$) and with 1.15 ± 0.14 mm in GOLD 4 ($p = 0.833$). WP₃₋₈ showed a similar trend as there were no significant differences between GOLD 0 and GOLD 1, the highest values were found in GOLD 2, while the values in GOLD 3 and GOLD 4 were again lower. TD₃₋₈ and LA₃₋₈ showed no significant differences between the GOLD stages (Figures 2, 4; Table 2).

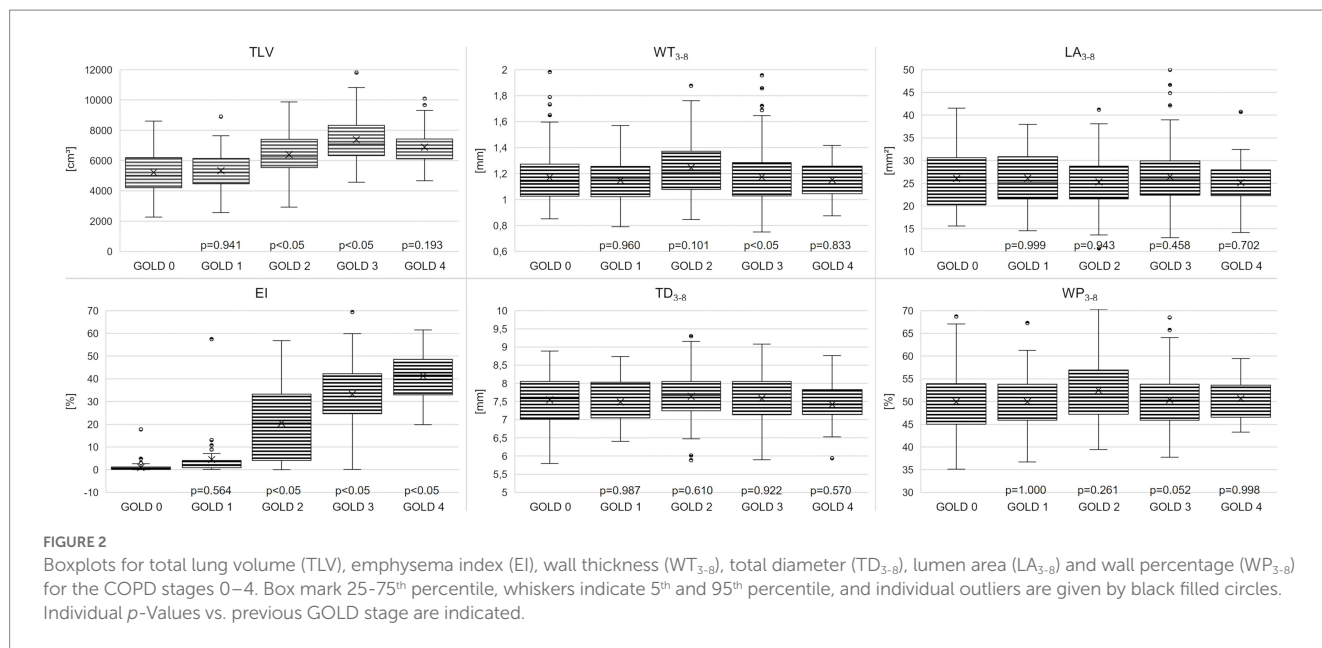
Lobe-based quantification of emphysema and airway disease

A lobe-based analysis was performed, whereby only lobes with a complete set of results for the airway generations 3rd–8th were included, which was the case for 913 out of the theoretical set of 2952 lobes. The lingula and middle lobe were excluded entirely due to a high number of missing results for individual generations. The lobe-based results

TABLE 1 Patient demographics and body plethysmography parameters.

	GOLD 0	GOLD 1	GOLD 2	GOLD 3	GOLD 4	pANOVA
N	123	33	115	181	40	-
Sex [f/m]	59/64	16/17	53/62	74/74	26/14	-
Age [y]	55 ± 15	63 ± 12*	63 ± 11	61 ± 10	64 ± 8	0.006
Height [cm]	1.71 ± 0.10	1.68 ± 0.11	1.68 ± 0.10	1.69 ± 0.08	1.66 ± 0.07	0.023
Weight [kg]	83 ± 19	79 ± 16	75 ± 18	72 ± 18	64 ± 12*	0.037
BMI	28 ± 5	28 ± 5	26 ± 5	25 ± 6	23 ± 4	0.001
TLC	6.2 ± 1.4	6.4 ± 1.7	7.8 ± 5.5	8.8 ± 4.5	8.1 ± 1.2	0.001
RV	2.6 ± 0.8	3.2 ± 1.5	4.8 ± 1.3*	5.8 ± 1.4*	5.4 ± 0.5	0.001
VC	3.6 ± 1.2	3.3 ± 1.2	2.4 ± 1.1*	2.7 ± 0.8	2.2 ± 0.8	0.001
FVC	3.5 ± 1.2	3.1 ± 1.2	2.2 ± 1.1*	2.3 ± 0.8	2.2 ± 0.9	0.001
FEV1 [L]	2.8 ± 0.9	2.2 ± 0.8	1.1 ± 0.6	0.9 ± 0.4	0.69 ± 0.23	<0.001
FEV1%pred	101.3 ± 6.4	88.3 ± 6.6	61.5 ± 9.7	41.7 ± 6.1	27.7 ± 2.3	<0.001
FEV1/FVC	0.8 ± 0.01	0.7 ± 0.1	0.5 ± 0.1	0.4 ± 0.1	0.28 ± 0.05	<0.001

Patient demographics (sex, age, height, weight, and BMI) and body plethysmography parameters total lung capacity (TLC), residual volume (RC), (vital capacity (VC) forced vital capacity (FVC), forced expiratory volume in 1 s (FEV1), FEV1 predicted (FEV1%), and FEV1/FVC ratio) are shown. All data are given as mean ± standard deviation. **p* < 0.05 vs. previous GOLD stage.



for GOLD 0 and 1, and GOLD 3 and 4 were combined into GOLD0/1 and GOLD3/4, respectively, to compensate for limited complete datasets. The lobe volume difference between GOLD 0/1 and GOLD 3/4 was higher in the upper lobes with a difference of 288 cm³ (+20%), than in the lower lobes with a difference of 162 cm³ (+10%). The EI showed no significant differences between upper and lower lobes in GOLD 1, while EI was higher in the upper lobes in GOLD 2 and GOLD3/4. The values for WP₃₋₈ showed different trends for the upper and lower lobes. In the upper lobes, WP₃₋₈ was overall lower than in the lower lobes and tended to be higher with increasing GOLD stages (*p* = 0.887, *p* = 0.928). In the lower lobes, WP₃₋₈ was 49.9 ± 6.5% in GOLD 0/1, higher in GOLD 2 with 51.9 ± 6.4% (*p* < 0.05) and tended to be lower in GOLD 3/4 with 51.0 ± 6.0%. In the upper lobes, TD₃₋₈ and LA₃₋₈ tended to be higher with higher GOLD stages (*p* = 0.201, *p* = 0.307). In the lower lobes LA₃₋₈ showed no significant differences,

while TD₃₋₈ had the highest values at GOLD 2 (*p* = 0.216, *p* = 0.866) (Figure 5; Table 3).

Emphysema and airway disease are independent factors of airflow limitation

TLC showed strong correlations with TLV for all GOLD stages (*r* = 0.79–0.86), low to moderate correlations with EI (*r* = 0.29–0.64), and weak to moderate correlations with WP₃₋₈ (*r* = -0.10 - -0.51). RV showed strong to correlations with TLV and EI for GOLD 0–4 (*r* = 0.71, *r* = 0.77), while the correlations with WP₃₋₈ were negligible to moderate (*r* = -0.04 - -0.54). The correlations between VC and TLV, EI and WP₃₋₈ were overall weak for GOLD 0–4 (*r* = -0.13–0.18). The correlation of FEV1%pred for GOLD 0–4 showed moderate

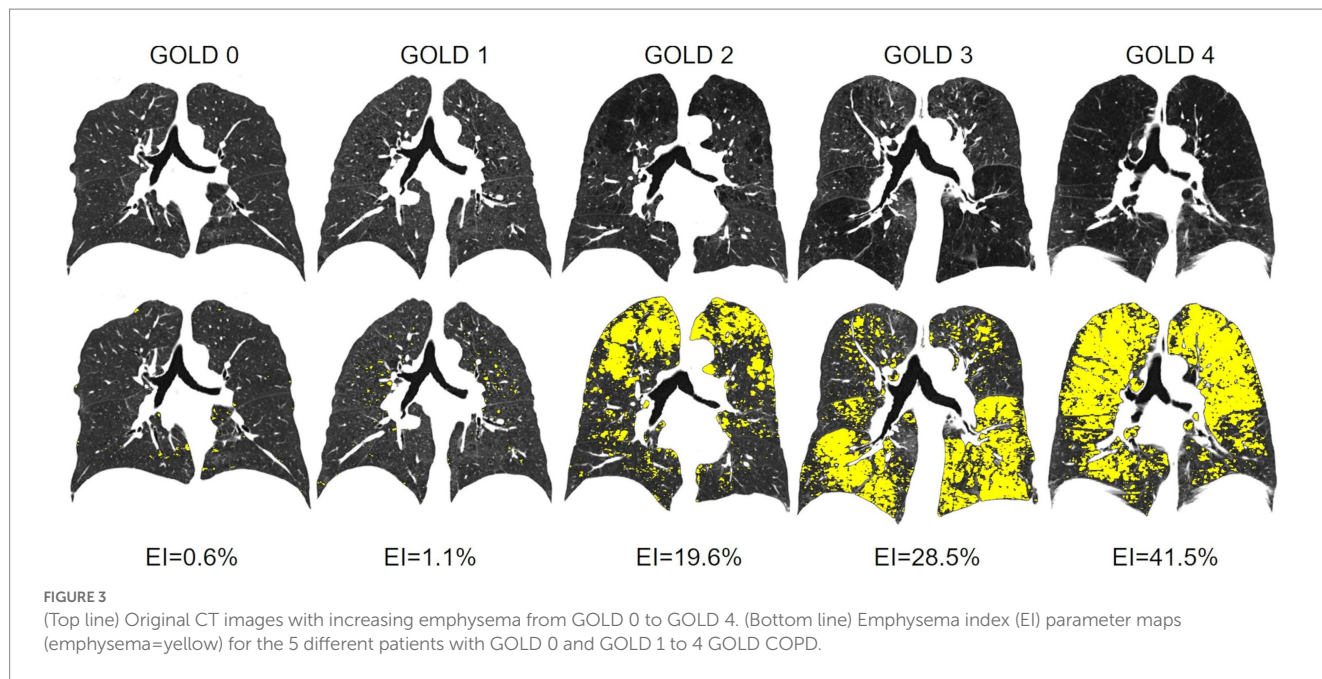


TABLE 2 QCT parameters for GOLD stages 0–4.

	GOLD 0	GOLD 1	GOLD 2	GOLD 3	GOLD 4	pANOVA
TLV [cm ³]	5198 ± 1349	5401 ± 1286	6353 ± 1368	7405 ± 1366	6892 ± 1292	<0.001
EI [%]	1.0 ± 1.8	4.5 ± 9.9	19.4 ± 15.8	32.7 ± 13.4	41.4 ± 10.0*	<0.001
MLD [HU]	-802 ± 38	-820 ± 32*	-850 ± 30	-872 ± 19	-876 ± 14	<0.001
WT ₃₋₈ [mm]	1.17 ± 0.21	1.14 ± 0.16	1.24 ± 0.24	1.17 ± 0.19	1.15 ± 0.14	<0.05
TD ₃₋₈ [mm]	7.54 ± 0.68	7.47 ± 0.55	7.63 ± 0.64	7.30 ± 0.66	7.42 ± 0.54	0.328
LA ₃₋₈ [mm ²]	26.05 ± 6.62	26.11 ± 6.07	25.47 ± 5.67	26.60 ± 6.05	25.16 ± 4.86	0.626
WP ₃₋₈ [%]	50.0 ± 7.2	49.8 ± 6.2	52.4 ± 7.2	50.3 ± 5.9	50.6 ± 4.6	<0.05

Total lung volume (TLV), emphysema index (EI) and mean lung density (MLD) as well as wall thickness (WT₃₋₈), total diameter (TD₃₋₈), lumen area (LA₃₋₈) and wall percentage (WP₃₋₈) were calculated. Generation-based results for WT, TD, LA, and WP were consolidated into one value (G₃₋₈). All data are given as mean ± standard deviation. **p* < 0.05 vs. previous GOLD stage.

correlations with TLV (*r* = -0.59, *p* = 0.001) and strong correlations with EI (*r* = 0.78, *p* = 0.002), while the correlations for the individual GOLD stages were low to moderate (*r* = -0.10–0.47). The correlation between FEV1%pred and WP₃₋₈ was negligible to moderate (*r* = 0.01–0.39) for GOLD 0–4 and all individual GOLD stages (Table 4; Supplementary Table 1).

Importantly, in a multilinear regression analysis the dependent variable FEV1%pred can be predicted by a combination of both the independent variables EI (*p* < 0.001) and WP₃₋₈ (*p* < 0.001), whereas the independent variables biological sex (*p* = 0.893) and age (*p* = 0.598) could not (Figure 6; Table 4).

Discussion

In this work, we demonstrate that emphysema and airway disease independently contribute to airflow limitation in COPD, in both high-risk patients and patients with COPD at GOLD stages 1–4, using QCT in 522 individuals studied with the same CT scanner and protocol. Second, we show that individual lobes show distinct differences of emphysema and airway disease at different GOLD stages with a

relatively higher emphysema values in the upper lobes compared to the lower lobes. Thus, we found typical values of EI and WP for each GOLD-stage.

Total lung volume (TLV) was higher in GOLD 3 than in GOLD 0, which is within expectations as emphysema progression is associated with hyperinflation. However, TLV was again lower in GOLD 4, which may represent scarring in advanced destructive emphysema, but could also be related to increased mortality with a selection bias. The EI increased across all GOLD stages, but only significantly between GOLD 1 and GOLD 2, and GOLD 2 and GOLD 3, suggesting that the severity of the emphysema progression may not be linear. This contradicts the assumption that emphysema progression might be accelerated in advanced COPD, since locally severely altered alveolar micromechanics within an injured lung might itself ‘become an independent trigger of lung injury progression’ (29, 30). The explanation may be that in GOLD 4, emphysema is nevertheless higher in relation to the remaining normal lung tissue, although the absolute difference between GOLD 3 and GOLD 4 is lower. Overall, our results are consistent with the literature in which QCT has been successfully used to detect the progression of emphysema (31, 32). MLD increased also significantly from GOLD 0 to GOLD 4, as MLD

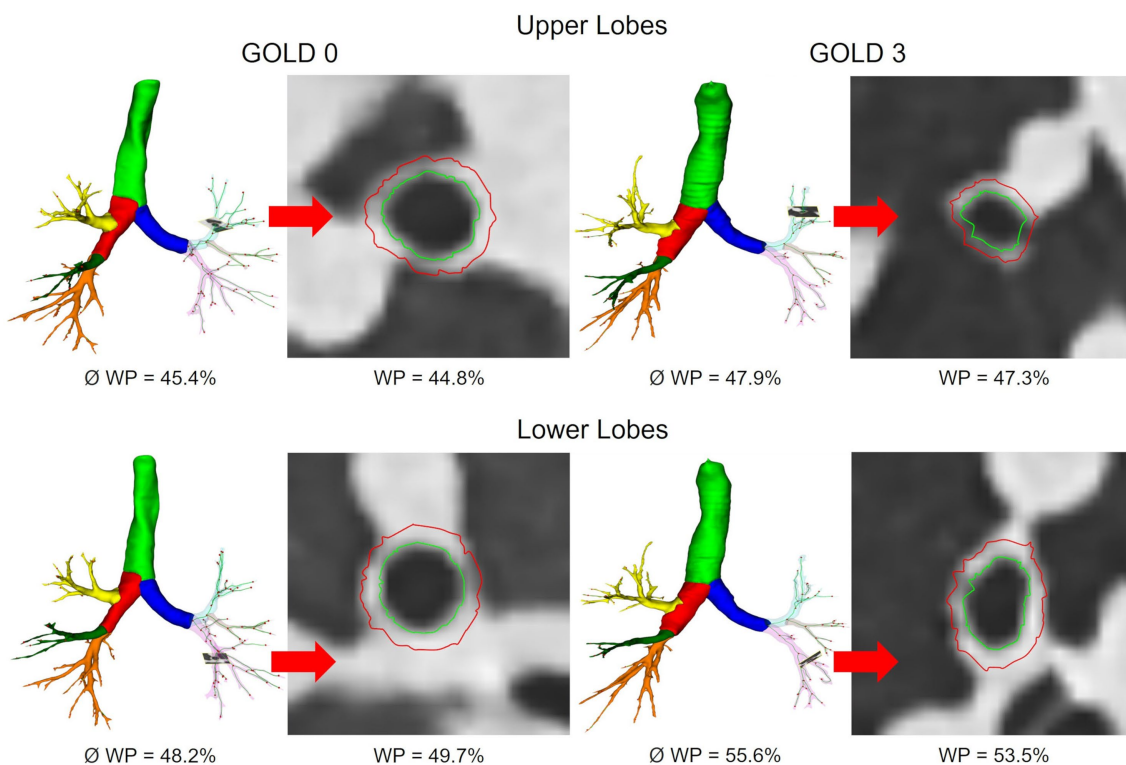


FIGURE 4 Segmented airway tree of the upper and lower lobes in GOLD 0 and GOLD 3. Average WP for the entire airway tree (\emptyset) and representative slices for individual bronchi are shown.

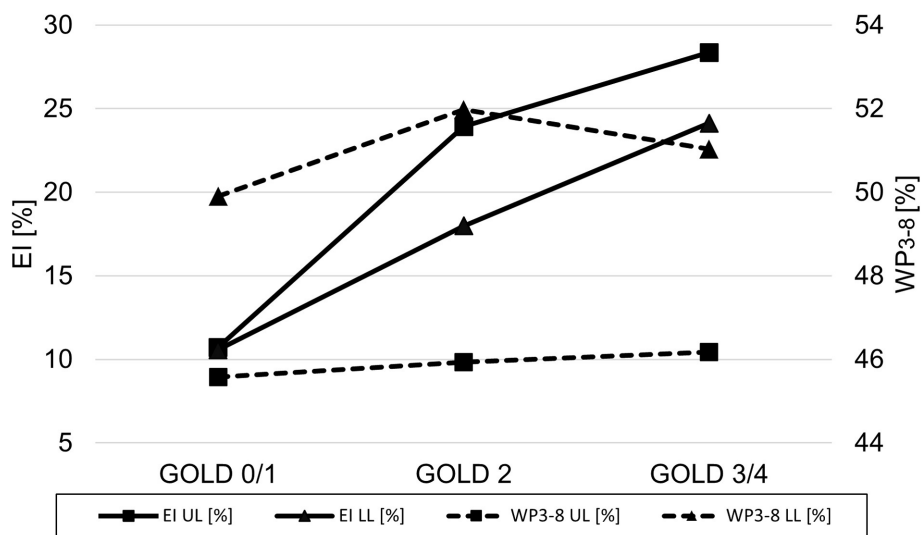


FIGURE 5 Line plot of emphysema index (■ EI) and wall percentage (--- WP₃₋₈) for GOLD 0/1, GOLD 2, and GOLD 3/4 for the upper lobes (UL=square) and the lower lobes (LL=triangle).

and EI are strongly correlated. In this context, it should be mentioned that MLD in advanced COPD is influenced by both emphysema and lung fibrotic changes, the latter might explain the slightly higher MLD values in GOLD 4 when compared with GOLD 3. The use of the parameter Perc15 can be helpful to overcome this problem.

WT₃₋₈ and WP₃₋₈ showed no relevant differences between GOLD 0 and GOLD 1, most likely because the disease-related changes may be too subtle for detection. WT₃₋₈ and WP₃₋₈ showed the highest values at GOLD 2, accompanied by higher TD₃₋₈ and a slightly lower LA₃₋₈, which could be explained by inflammatory swelling of the

TABLE 3 QCT parameters for the combined upper and lower lobes at different GOLD stages.

	GOLD 0/1	GOLD 2	GOLD 3/4	pANOVA
Upper lobes				
N	124	74	120	–
ULV [cm ³]	1140 ± 387	1355 ± 437*	1428 ± 546	<0.001
EI [%]	11.0 ± 17.8	24.5 ± 17.6*	27.7 ± 22.5	<0.001
MLD [HU]	–833 ± 41	–864 ± 29*	–864 ± 39	<0.001
WT ₃₋₈ [mm]	1.10 ± 0.17	1.14 ± 0.21	1.15 ± 0.20	0.014
TD ₃₋₈ [mm]	7.86 ± 0.95	8.07 ± 1.07	8.25 ± 1.00	<0.05
LA ₃₋₈ [mm ²]	32.01 ± 10.68	33.78 ± 10.58	36.40 ± 13.41	<0.05
WP ₃₋₈ [%]	45.6 ± 5.7	46.0 ± 5.0	46.0 ± 5.8	0.824
Lower lobes				
N	211	134	250	–
LLV [cm ³]	1358 ± 422	1392 ± 476	1520 ± 482*	<0.001
EI [%]	11.0 ± 18.1	18.1 ± 17.2*	24.0 ± 19.1*	<0.001
MLD [HU]	–816 ± 51	–837 ± 41*	–845 ± 46	<0.001
WT ₃₋₈ [mm]	1.27 ± 0.20	1.35 ± 0.24	1.30 ± 0.23	<0.05
TD ₃₋₈ [mm]	8.33 ± 0.94	8.48 ± 0.95	8.41 ± 0.86	0.373
LA ₃₋₈ [mm ²]	31.93 ± 9.98	31.79 ± 9.02	31.79 ± 8.14	0.924
WP ₃₋₈ [%]	49.9 ± 6.5	51.9 ± 6.4	51.0 ± 6.0	<0.05

Lobe volumes for the upper (ULV) and lower lobes (LLV), emphysema index (EI) and mean lung density (MLD), wall thickness (WT₃₋₈), total diameter (TD₃₋₈), lumen area (LA₃₋₈), and wall percentage (WP₃₋₈) are shown. All data are given as mean ± standard deviation. **p* < 0.05 vs. previous GOLD stage.

airway walls in the process of bronchitis. This observation is supported by the literature, which recognizes small airway disease as a central feature of COPD, with increasing narrowing and destruction of the small airways representing a mixture of chronic inflammation (28, 33, 34). In this context, Koo et al. demonstrated significant loss of terminal and transitional bronchioles in patients with GOLD 1 and GOLD 2, as the remaining small airways had thickened walls and narrowed lumens that were also present in regions with no emphysema (8).

However, in contrast to parts of the literature, WT₃₋₈, WP₃₋₈ and TD₃₋₈ tended to be lower in GOLD 3 and GOLD 4, while LA₃₋₈ was higher in GOLD 3 and again lower in GOLD 4. These changes may be interpreted as a possible transition from reversible airway inflammation to irreversible airway damage with airway wall degradation. This theory is supported by Smith et al., who observed significantly reduced airway wall thickness in most areas of the central tracheobronchial tree in COPD patients (35). They hypothesize that possible mechanisms include airway smooth muscle regression, apoptosis or replacement fibrosis resulting from chronic airway inflammation, and decreased bronchial vascular volume (36, 37). In addition, increasing emphysematous destruction of the lung parenchyma appears to have a significant impact on airway dimensions (38). In detail, emphysema leads to destruction of the lung parenchyma, resulting in loss of lung attachments that stabilize the airways and prevent them from collapse. Therefore, an increase in emphysema should result in partial airway collapse and thus a decrease in LA and TD, whereas WT and WP, unless the airway wall mass itself has not changed, should increase. On the other hand, hyperinflation leads to an increase in lung volume, stretching the airways and most likely increasing LA and TD and decreasing WT

and WP, having a partially opposing effects on the airways. In our cohort, the reduction of LA₃₋₈ in GOLD 4 might contribute to the destabilizing effects of emphysema.

We paid attention to potential regional differences within the lung by analysing individual lung lobes. EI was significantly higher in both upper lobes, resulting in greater volume increase due to emphysematous hyperinflation, consistent with the literature. (39). The spatial differences in airway involvement have been investigated in only a few studies. The COPD Gene Investigators reported that there were no differences in airway wall thickness or Pi10 between patients with predominant lower and predominant upper lobe emphysema, although the former group had greater airflow limitation and more air-trapping (40). Park et al. showed that patients with predominant lower lobe emphysema showed greater airway involvement than those with predominant upper lobe emphysema, possibly leading to more frequent exacerbations and poorer response to therapy (41). In accordance with Park et al., our results also showed significant higher WP₃₋₈ in the lower lobes. However, looking at the pooled results for GOLD 0/1, GOLD 2, and GOLD 3/4, we see that WP₃₋₈ was higher in the upper lobes with increasing GOLD stages, while in the lower lobes it was the highest in GOLD 2 and again lower in GOLD 3/4. Interestingly, we would have expected a lower WP₃₋₈ in higher GOLD stages in the upper lobes, as advanced emphysema should be associated with airway degeneration and collapse. One possible explanation may be the pooling of GOLD 3 and GOLD 4 data, which was necessary because airway segmentation becomes more difficult as disease progresses. Another reason could be the initial differences in WP₃₋₈ between upper and lower lobes, which may influence the changes of airway dimensions in relation to the GOLD stage.

TABLE 4 Spearman rank order correlation coefficient for lung function parameters and QCT.

	GOLD 0–4	GOLD 0	GOLD 1	GOLD 2	GOLD 3	GOLD 4
TLC						
TLV [cm ³]	0.86 (0.001)	0.83 (0.001)	0.79 (0.001)	0.78 (0.001)	0.81 (0.001)	0.83 (0.001)
EI [%]	0.56 (0.001)	0.29 (0.001)	0.64 (0.001)	0.26 (0.001)	0.27 (0.001)	0.17 (0.399)
WP ₃₋₈ [%]	-0.12 (0.012)	-0.11 (0.245)	-0.51 (0.002)	-0.17 (0.078)	-0.10 (0.165)	-0.25 (0.211)
RV						
TLV [cm ³]	0.71 (0.001)	0.38 (0.001)	0.48 (0.001)	0.56 (0.001)	0.65 (0.001)	0.43 (0.297)
EI [%]	0.77 (0.001)	0.10 (0.271)	0.69 (0.001)	0.56 (0.001)	0.35 (0.001)	0.49 (0.286)
WP ₃₋₈ [%]	-0.04 (0.386)	-0.07 (0.392)	-0.28 (0.118)	-0.16 (0.089)	-0.08 (0.252)	-0.54 (0.297)
VC						
TLV [cm ³]	0.18 (0.001)	0.73 (0.001)	0.63 (0.001)	0.33 (0.001)	0.81 (0.001)	0.47 (0.001)
EI [%]	-0.38 (0.001)	0.25 (0.001)	0.1 (0.577)	-0.28 (0.001)	0.27 (0.001)	0.16 (0.331)
WP ₃₋₈ [%]	-0.13 (0.001)	-0.09 (0.329)	-0.29 (0.101)	-0.08 (0.411)	-0.11 (0.165)	-0.05 (0.725)
FEV1%pred						
TLV [cm ³]	-0.59 (0.001)	-0.1 (0.271)	-0.02 (0.926)	-0.31 (0.001)	-0.15 (0.042)	0.26 (0.658)
EI [%]	-0.78 (0.001)	-0.16 (0.069)	-0.18 (0.311)	-0.43 (0.001)	-0.13 (0.076)	-0.71 (0.136)
WP ₃₋₈ [%]	0.01 (0.883)	0.01 (0.933)	0.39 (0.025)	0.04 (0.665)	0.02 (0.754)	0.31 (0.564)

Spearman rank order correlation coefficient were calculated for total lung volume (TLV), emphysema index (EI) and wall percentage (WP) with total lung capacity (TLC), residual volume (RV), vital capacity (VC) and FEV1%predicted (FEV1%pred).

In our study cohort, strong correlations between parenchymal QCT and whole-body plethysmography parameters were observed. The QCT parameter TLV, which increased from GOLD stage 0 to 3, showed strong correlations with TLC determined by whole-body plethysmography, which has already been described (42). TLV showed also low to moderate correlations with EI as emphysema progression is associated with hyperinflation. The residual volume (RV) showed strong correlations with TLV and EI for GOLD 0–4, as the main volume that increases with COPD severity is RV (43). The correlations between vital capacity (VC) and the CT parameters TLV, EI were weak for GOLD 0–4. The correlation between FEV1%pred and TLV as well as EI was strong since its connection is well established in the literature (44). In comparison whole-body plethysmography parameters TLC, RC and VC showed at best weak correlations with QCT airway parameters. However, WP₃₋₈ in GOLD 1 and EI in GOLD 4 appeared to correlate better with FEV1%pred, suggesting that FEV1 impairment may be more attributable to airway disease in the lower GOLD stages and more to emphysema in the higher GOLD stages. This may also be reflected in previous observations in the COPD Gene study, demonstrating that small airways disease increases only from GOLD 0 to GOLD 4, and declines thereafter, whereas emphysema increases with every GOLD stage. Of note, results from larger airway analyses as in our present study can be regarded as surrogates for processes in the small airways not visible at CT (45). Restrictively, this observation may also be to selection bias since the patient numbers in GOLD 1 and GOLD 4 were relatively low. However, this observation also highlights the limitations of FEV1, as it is influenced by at least two very different pathophysiological mechanisms, namely airway wall thickening for inflammation (also in vessels) and attachment disruption (and vascular disruption) for protease activity in emphysema. In this study, this was also shown with multilinear regression, where the dependent variable FEV1%pred can be predicted by a linear combination of the two independent variables EI and WP₃₋₈. There was no association with biological sex and age,

which can be expected since FEV1% predicted is already normalized by the age, sex and other factors. However, emphysema, airway wall thickness (WT), total diameter (TD), and lumen area (LA) are dependent on sex and age (46, 47). In this context, it should be emphasized that other lung function parameters such as DCLO or FRC may be better suited to describe the different contributions of emphysema and airway disease, as already shown in the literature (48).

Our study has some limitations. The interpretation of quantitative parameters should be done carefully, as subtle changes may be due to noise or measurement errors. We tried to reduce technical confounders by using the same scanner, slice thickness, and reconstruction kernels. In our study cohort a dose-modulated protocol was used with a reference of 120 kV/70 mA (n = 180) or 100 kV/117 mA (n = 312), which may influence the results. However, two phantom based studies analysed the influence on the acquisition parameters current time product (mA) and tube potential (kV) on YACTAs QCT parameters (17, 49). The acquisition parameters used in the phantom study were not identical with 120 kV/60 mA and 80 kV/120 mA, but somehow comparable in their variance to each other. The comparison of the two protocols showed no significant differences, for example for MLD with -923.4 ± 6.4 HU vs. -923.2 ± 6.4 HU or for WP% with $43.3 \pm 6.9\%$ vs. $43.6 \pm 7.2\%$ (17, 49). However, the exact influence of the different protocols is difficult to quantify, and possible confounders cannot be completely excluded, although the use of both protocols in each GOLD group should weaken any possible effect. Other important confounders are the variation of lung volume and cigarette smoking status (9). The variation of lung volume was reduced as best as possible by instructing and monitoring all patients for a stable full inspiratory position. Smoking status was not considered because consistent smoking history was not available for all patients. This can be considered a substantial weakness, since cigarette smoking status influences the

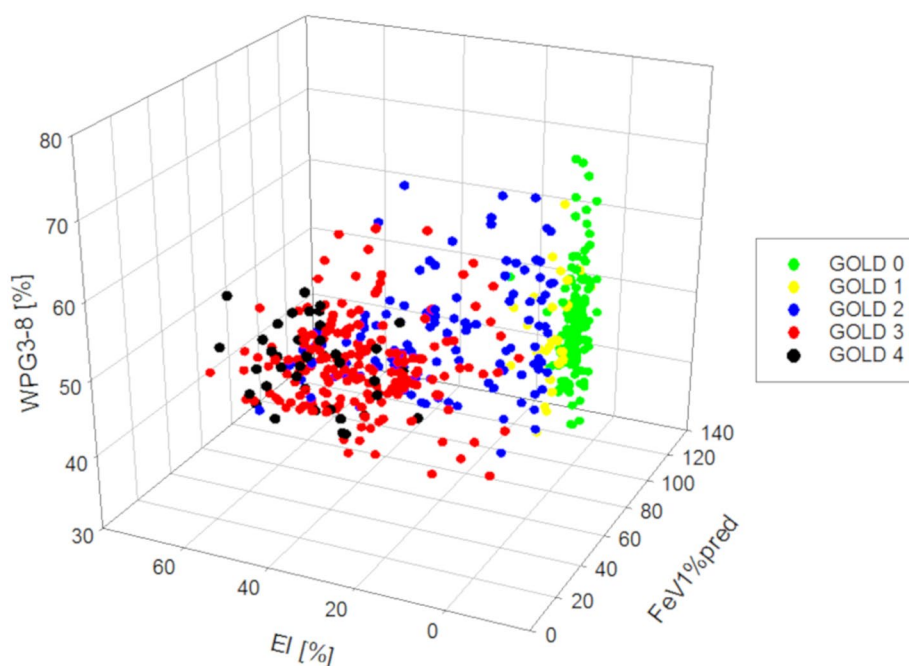


FIGURE 6
3D-residual scatterplots for the dependent variable FEV1%pred and the independent variables EI and WP₃₋₈.

quantification of emphysema and airway disease (4, 50). Several authors have shown that current smokers have higher lung density, presumably due to a smoking-related increase in inflammatory cells in the lungs of current smokers, whereas other studies have shown that bronchial dimensions depend on current smoking status (51–54). However, in a large study from Rotterdam of approximately 2000 COPD patients, 41% were current smokers and 57.6% were former smokers or never smokers, indicating a relatively even distribution in an unselected population. Assuming a similar distribution in our study cohort, the impact of smoking on QCT parameters should be limited within each GOLD group. Although we agree that smoking status would have increased data quality, we still consider the results robust in the context of a descriptive cross-sectional study.

This work focused on QCT for GOLD stage-specific quantification of emphysema and airway disease. QCT parameters showed significant differences for GOLD 0–4 COPD, while lung lobe analysis revealed significant differences in the changes of airway dimensions between upper and lower lobes. The observed changes in airway dimensions may indicate airway inflammation in GOLD 2, which may lead to irreversible airway destruction in GOLD 3 and GOLD 4. Emphysema and airway disease both contribute independently to lung function decline. However, COPD is a very heterogeneous disease, which means that different stages of airway disease may coexist in the same lung, emphasizing the need to assess the spatial distribution within the lung.

Data availability statement

The raw data supporting the conclusions of this article will be made available by the authors, without undue reservation.

Ethics statement

The studies involving human participants were reviewed and approved by Ethics committee of the University of Heidelberg. The patients/participants provided their written informed consent to participate in this study.

Author contributions

PK, CB, MK, WW, OW, CH, FH, FT, H-UK, and MW contributed study concept, design, and acquisition, analysis and interpretation of the data. OW developed the software used in this work. All authors contributed to the article and approved the submitted version.

Funding

This study was supported by grants from the Bundesministerium für Bildung und Forschung (BMBF) to the German Center for Lung Research (DZL) (82DZL004A and 82DZL004A2). For the publication fee we acknowledge financial support by Deutsche Forschungsgemeinschaft within the funding programme Open Access Publikationskosten as well as by Heidelberg University.

Acknowledgments

We thank all patients for their participation in this study. This work contains parts of the thesis of Christian Brunner.

Conflict of interest

The authors declare that the research was conducted in the absence of any commercial or financial relationships that could be construed as a potential conflict of interest.

Publisher's note

All claims expressed in this article are solely those of the authors and do not necessarily represent those of their affiliated

organizations, or those of the publisher, the editors and the reviewers. Any product that may be evaluated in this article, or claim that may be made by its manufacturer, is not guaranteed or endorsed by the publisher.

Supplementary material

The Supplementary material for this article can be found online at: <https://www.frontiersin.org/articles/10.3389/fmed.2023.1184784/full#supplementary-material>

References

- Mathers CD, Loncar D. Projections of global mortality and burden of disease from 2002 to 2030. *PLoS Med.* (2006) 3:e442. doi: 10.1371/journal.pmed.0030442
- Rabe KF, Hurd S, Anzueto A, Barnes PJ, Buist SA, Calverley P, et al. Global strategy for the diagnosis, management, and prevention of chronic obstructive pulmonary disease: Gold executive summary. *Am J Respir Crit Care Med.* (2007) 176:532–55. doi: 10.1164/rccm.200703-456SO
- Vogelmeier CF, Criner GJ, Martinez FJ, Anzueto A, Barnes PJ, Bourbeau J, et al. Global strategy for the diagnosis, management, and prevention of chronic obstructive lung disease 2017 report. Gold executive summary. *Am J Respir Crit Care Med.* (2017) 195:557–82. doi: 10.1164/rccm.201701-0218PP
- Jobst BJ, Weinheimer O, Buschulte T, Trauth M, Tremper J, Delorme S, et al. Longitudinal airway remodeling in active and past smokers in a lung Cancer screening population. *Eur Radiol.* (2019) 29:2968–80. doi: 10.1007/s00330-018-5890-4
- Takayanagi S, Kawata N, Tada Y, Ikari J, Matsuura Y, Matsuoka S, et al. Longitudinal changes in structural abnormalities using Mdc1 in Copd: do the Ct measurements of Airway Wall thickness and small pulmonary vessels change in parallel with emphysematous progression? *Int J Chron Obstruct Pulmon Dis.* (2017) 12:551–60. doi: 10.2147/copd.S121405
- Regan EA, Lynch DA, Curran-Everett D, Curtis JL, Austin JH, Grenier PA, et al. Clinical and radiologic disease in smokers with Normal spirometry. *JAMA Intern Med.* (2015) 175:1539–49. doi: 10.1001/jamainternmed.2015.2735
- Jimborean G, Ianoși ES, Postolache P, Arghir O. The role of quantitative computed tomography in the diagnosis of chronic obstructive pulmonary disease. *Pneumologia.* (2016) 65:184–8.
- Koo HK, Vasilescu DM, Booth S, Hsieh A, Katsamenis OL, Fishbane N, et al. Small airways disease in mild and moderate chronic obstructive pulmonary disease: a cross-sectional study. *Lancet Respir Med.* (2018) 6:591–602. doi: 10.1016/S2213-2600(18)30196-6
- Lynch DA, Al-Qaisi MA. Quantitative computed tomography in chronic obstructive pulmonary disease. *J Thorac Imaging.* (2013) 28:284–90. doi: 10.1097/RTI.0b013e318298733c
- Coxson HO, Leipsic J, Parraga G, Sin DD. Using pulmonary imaging to move chronic obstructive pulmonary disease beyond Fv1. *Am J Respir Crit Care Med.* (2014) 190:135–44. doi: 10.1164/rccm.201402-0256PP
- Labaki WW, Martinez CH, Martinez FJ, Galbán CJ, Ross BD, Washko GR, et al. The role of chest computed tomography in the evaluation and Management of the Patient with chronic obstructive pulmonary disease. *Am J Respir Crit Care Med.* (2017) 196:1372–9. doi: 10.1164/rccm.201703-0451PP
- Lynch DA, Austin JH, Hogg JC, Grenier PA, Kauczor HU, Bankier AA, et al. Ct-definable subtypes of chronic obstructive pulmonary disease: a statement of the Fleischner society. *Radiology.* (2015) 277:141579:192–205. doi: 10.1148/radiol.2015141579
- Gevenois PA, De Vuyst P, de Maertelaer V, Zanen J, Jacobovitz D, Cosio MG, et al. Comparison of computed density and microscopic morphometry in pulmonary emphysema. *Am J Respir Crit Care Med.* (1996) 154:187–92. doi: 10.1164/ajrccm.154.1.8680679
- Madani A, Zanen J, Maertelaer V, Gevenois PA. Pulmonary emphysema: objective quantification at multi-detector row Ct—comparison with macroscopic and microscopic morphometry. *Radiology.* (2006) 238:1036–43. doi: 10.1148/radiol.2382042196
- Hackx M, Bankier AA, Gevenois PA. Chronic obstructive pulmonary disease: Ct quantification of airways disease. *Radiology.* (2012) 265:34–48. doi: 10.1148/radiol.12111270
- Nakano Y, Wong JC, de Jong PA, Buzatu L, Nagao T, Coxson HO, et al. The prediction of small airway dimensions using computed tomography. *Am J Respir Crit Care Med.* (2005) 171:142–6. doi: 10.1164/rccm.200407-874OC
- Leutz-Schmidt P, Wielputz MO, Skornitzke S, Weinheimer O, Kauczor HU, Puderbach MU, et al. Influence of acquisition settings and radiation exposure on Ct lung densitometry—an anthropomorphic ex vivo phantom study. *PLoS One.* (2020) 15:e0237434. doi: 10.1371/journal.pone.0237434
- Halpin DMG, Criner GJ, Papi A, Singh D, Anzueto A, Martinez FJ, et al. Global initiative for the diagnosis, management, and prevention of chronic obstructive lung disease. The 2020 Gold science committee report on Covid-19 and chronic obstructive pulmonary disease. *Am J Respir Crit Care Med.* (2021) 203:24–36. doi: 10.1164/rccm.202009-3533SO
- Cooper BG, Stocks J, Hall GL, Culver B, Steenbruggen I, Carter KW, et al. The global lung function initiative (Gli) network: bringing the World's respiratory reference values together. *Breathe.* (2017) 13:e56–e64. doi: 10.1183/20734735.012717
- Kauczor HU, Wielputz MO, Owsijewitsch M, Ley-Zaporozhan J. Computed tomographic imaging of the Airways in Copd and Asthma. *J Thorac Imaging.* (2011) 26:290–300. doi: 10.1097/RTI.0b013e3182277113
- Wielputz MO, Weinheimer O, Eichinger M, Wiebel M, Biederer J, Kauczor HU, et al. Pulmonary emphysema in cystic fibrosis detected by densitometry on chest multidetector computed tomography. *PLoS One.* (2013) 8:e73142. doi: 10.1371/journal.pone.0073142
- Weinheimer O, Wielputz MO, Konietzke P, Heussel CP, Kauczor HU, Brochhausen C, et al. Fully automated lobe-based airway taper index calculation in a low dose Mdc1 Ct study over 4 time-points. *Image Proc.* (2017) 10133:242–50. doi: 10.1117/12.2254387
- Konietzke P, Weinheimer O, Wielputz MO, Savage D, Ziyeh T, Tu C, et al. Validation of automated lobe segmentation on paired inspiratory-expiratory chest Ct in 8-14 year-old children with cystic fibrosis. *PLoS One.* (2018) 13:e0194557. doi: 10.1371/journal.pone.0194557
- Wielputz MO, Eichinger M, Weinheimer O, Ley S, Mall MA, Wiebel M, et al. Automatic airway analysis on multidetector computed tomography in cystic fibrosis: correlation with pulmonary function testing. *J Thorac Imaging.* (2013) 28:104–13. doi: 10.1097/RTI.0b013e3182765785
- Weinheimer O, Achenbach T, Düber C. Fully automated extraction of airways from Ct scans based on self-adapting region growing. *Computerized Tomography.* (2009) 27:64–74.
- Weinheimer O, Achenbach T, Bletz C, Düber C, Kauczor HU, Heussel CP. About objective 3-D analysis of airway geometry in computerized tomography. *IEEE Trans Med Imaging.* (2008) 27:64–74. doi: 10.1109/TMI.2007.902798
- Schober P, Boer C, Schwarte LA. Correlation coefficients: appropriate use and interpretation. *Anesth Analg.* (2018) 126:1763–8. doi: 10.1213/ANE.0000000000002864
- Nakano Y, Muro S, Sakai H, Hirai T, Chin K, Tsukino M, et al. Computed tomographic measurements of airway dimensions and emphysema in smokers. Correlation with lung function. *Am J Respir Crit Care Med.* (2000) 162:1102–8. doi: 10.1164/ajrccm.162.3.9907120
- Knudsen L, Ochs M. The micromechanics of lung alveoli: structure and function of surfactant and tissue components. *Histochem Cell Biol.* (2018) 150:661–76. doi: 10.1007/s00418-018-1747-9
- Konietzke P, Wielputz MO, Wagner WL, Wuennemann F, Kauczor HU, Heussel CP, et al. Quantitative Ct detects progression in Copd patients with severe emphysema in a 3-month interval. *Eur Radiol.* (2020) 30:2502–12. doi: 10.1007/s00330-019-06577-y
- Cavigli E, Camiciottoli G, Diciotti S, Orlandi I, Spinelli C, Meoni E, et al. Whole-lung densitometry versus visual assessment of emphysema. *Eur Radiol.* (2009) 19:1686–92. doi: 10.1007/s00330-009-1320-y
- Stolk J, Putter H, Bakker EM, Shaker SB, Parr DG, Piitulainen E, et al. Progression parameters for emphysema: a clinical investigation. *Respir Med.* (2007) 101:1924–30. doi: 10.1016/j.rmed.2007.04.016

33. Hasegawa M, Nasuhara Y, Onodera Y, Makita H, Nagai K, Fuke S, et al. Airflow limitation and airway dimensions in chronic obstructive pulmonary disease. *Am J Respir Crit Care Med.* (2006) 173:1309–15. doi: 10.1164/ajrccm.200601-037OC
34. Hogg JC, Macklem PT, Thurlbeck WM. Site and nature of airway obstruction in chronic obstructive lung disease. *N Engl J Med.* (1968) 278:1355–60. doi: 10.1056/NEJM196806202782501
35. Smith BM, Hoffman EA, Rabinowitz D, Bleecker E, Christenson S, Couper D, et al. Comparison of spatially matched airways reveals thinner airway walls in Copd. The multi-ethnic study of atherosclerosis (Mesa) Copd study and the subpopulations and intermediate outcomes in Copd study (Spiromics). *Thorax.* (2014) 69:987–96. doi: 10.1136/thoraxjnl-2014-205160
36. Cosio M, Ghezzo H, Hogg JC, Corbin R, Loveland M, Dosman J, et al. The relations between structural changes in small airways and pulmonary-function tests. *N Engl J Med.* (1978) 298:1277–81. doi: 10.1056/nejm197806082982303
37. Thurlbeck WM, Pun R, Toth J, Frazer RG. Bronchial cartilage in chronic obstructive lung disease. *Am Rev Respir Dis.* (1974) 109:73–80. doi: 10.1164/arrd.1974.109.1.73
38. Diaz AA, Estépar RSJ, Washko GR. Computed tomographic airway morphology in chronic obstructive pulmonary disease. Remodeling or innate anatomy? *Ann Am Thorac Soc.* (2016) 13:4–9. doi: 10.1513/AnnalsATS.201506-371PP
39. Takahashi M, Fukuoka J, Nitta N, Takazakura R, Nagatani Y, Murakami Y, et al. Imaging of pulmonary emphysema: a pictorial review. *Int J Chron Obstruct Pulmon Dis.* (2008) 3:193–204. doi: 10.2147/copd.s2639
40. Boueiz A, Chang Y, Cho MH, Washko GR, San José Estépar R, Bowler RP, et al. Lobar emphysema distribution is associated with 5-year radiological disease progression. *Chest.* (2018) 153:65–76. doi: 10.1016/j.chest.2017.09.022
41. Park J, Kim EK, Lee SH, Kim MA, Kim JH, Lee SM, et al. Phenotyping Copd patients with emphysema distribution using quantitative Ct measurement; more severe airway involvement in lower dominant emphysema. *Int J Chron Obstruct Pulmon Dis.* (2022) 17:2013–25. doi: 10.2147/copd.S362906
42. Mets OM, de Jong PA, van Ginneken B, Gietema HA, Lammers JW. Quantitative computed tomography in Copd: possibilities and limitations. *Lung.* (2012) 190:133–45. doi: 10.1007/s00408-011-9353-9
43. Cooper CB. The connection between chronic obstructive pulmonary disease symptoms and hyperinflation and its impact on exercise and function. *Am J Med.* (2006) 119:21–31. doi: 10.1016/j.amjmed.2006.08.004
44. Oh AS, Baraghoshi D, Lynch DA, Ash SY, Crapo JD, Humphries SM. Emphysema progression at Ct by deep learning predicts functional impairment and mortality: results from the Copdgene study. *Radiology.* (2022) 304:672–9. doi: 10.1148/radiol.213054
45. Bhatt SP, Soler X, Wang X, Murray S, Anzueto AR, Beaty TH, et al. Association between functional small airway disease and Fev1 decline in chronic obstructive pulmonary disease. *Am J Respir Crit Care Med.* (2016) 194:178–84. doi: 10.1164/rccm.201511-2219OC
46. Kim SS, Jin GY, Li YZ, Lee JE, Shin HS. Ct quantification of lungs and airways in normal Korean subjects. *Korean J Radiol.* (2017) 18:739–48. doi: 10.3348/kjr.2017.18.4.739
47. Copley SJ, Giannarou S, Schmid VJ, Hansell DM, Wells AU, Yang GZ. Effect of aging on lung structure in vivo: assessment with Densitometric and fractal analysis of high-resolution computed tomography data. *J Thorac Imaging.* (2012) 27:366–71. doi: 10.1097/RTL.0b013e31825148c9
48. Barjaktarevic I, Springmeyer S, Gonzalez X, Sirokman W, Coxson HO, Cooper CB. Diffusing capacity for carbon monoxide correlates best with tissue volume from quantitative Ct scanning analysis. *Chest.* (2015) 147:1485–93. doi: 10.1378/chest.14-1693
49. Leutz-Schmidt P, Weinheimer O, Jobst BJ, Dinkel J, Biederer J, Kauczor HU, et al. Influence of exposure parameters and iterative reconstruction on automatic airway segmentation and analysis on MdcT-an ex vivo phantom study. *PLoS One.* (2017) 12:e0182268. doi: 10.1371/journal.pone.0182268
50. Jobst BJ, Triphan SM, Sedlaczek O, Anjorin A, Kauczor HU, Biederer J, et al. Functional lung Mri in chronic obstructive pulmonary disease: comparison of T1 mapping, oxygen-enhanced T1 mapping and dynamic contrast enhanced perfusion. *PLoS One.* (2015) 10:e0121520. doi: 10.1371/journal.pone.0121520
51. Camiciottoli G, Cavigli E, Grassi L, Diciotti S, Orlandi I, Zappa M, et al. Prevalence and correlates of pulmonary emphysema in smokers and former smokers. A Densitometric study of participants in the Italung trial. *Eur Radiol.* (2009) 19:58–66. doi: 10.1007/s00330-008-1131-6
52. Grydeland TB, Dirksen A, Coxson HO, Pillai SG, Sharma S, Eide GE, et al. Quantitative computed tomography: emphysema and Airway Wall thickness by sex, age and smoking. *Eur Respir J.* (2009) 34:858–65. doi: 10.1183/09031936.00167908
53. Ashraf H, Lo P, Shaker SB, de Bruijne M, Dirksen A, Tønnesen P, et al. Short-term effect of changes in smoking behaviour on emphysema quantification by Ct. *Thorax.* (2011) 66:55–60. doi: 10.1136/thx.2009.132688
54. Jobst BJ, Weinheimer O, Trauth M, Becker N, Motsch E, Groß ML, et al. Effect of smoking cessation on quantitative computed tomography in smokers at risk in a lung Cancer screening population. *Eur Radiol.* (2018) 28:807–15. doi: 10.1007/s00330-017-5030-6

Glossary

ANOVA	One-way analysis of variance
COPD	Chronic obstructive pulmonary disease
CT	computed tomography
EI	emphysema index
FEV1	Forced Expiratory Pressure in 1 Second
FEV1%pre	FEV1 predicted
GOLD	Global Initiative for Obstructive Lung Disease
HU	Hounsfield units
LA	Lumen area
LLi	Lingula
LLL	Left lower lobe
LUL	Left upper lobe
RML	Middle lobe
RLL	Right lower lobe
RUL	Right upper lobe
MLD	Mean lung density
PFT	Pulmonary function test
QCT	Quantitative computed tomography
RV	Residual volume
SAD	Small airway disease
TD	Total diameter
TLC	Total lung capacity
TLV	Total lung volume
VC	Vital capacity
WP	Wall percentage
WT	Wall thickness